

Micro – Macro structural analysis of textile composite parts

Stepan V. Lomov, Björn Van Den Broucke, Ferruh Tümer, Ignaas Verpoest,
Laurent Dufort*, Patric de Luca*

Department MTM, Katholieke Universiteit Leuven, Kasteelpark Arenberg, 44 B-3001 Leuven (Heverlee) Belgium
Stepan.Lomov@mtm.kuleuven.ac.be

* ESI Software; 84, boulevard Vivier-Merle, 69485 LYON Cedex 03 France

ABSTRACT

The micro-macro calculation chain (draping simulation – local shear – local textile geometry – local stiffness of the composite – structural finite element analysis (FEA) of the part) is validated against experimental measurements at local (shear angles and local strains) and on global (load-deflection curve) levels. The results are also compared with FEA based on classical laminate theory calculation of local material properties.

1 INTRODUCTION

Development of validated predictive tools for mechanical performance of textile composite parts is a key issue for the composites industry. Such a tool must take into account variability of local properties of the composite, as a 3D textile preform undergoes shear deformations in the processing. The intensity of shear varies from point to point, changing the local properties of the composite part. We use the following “road map” (Figure 1) to link micro and macro calculations.

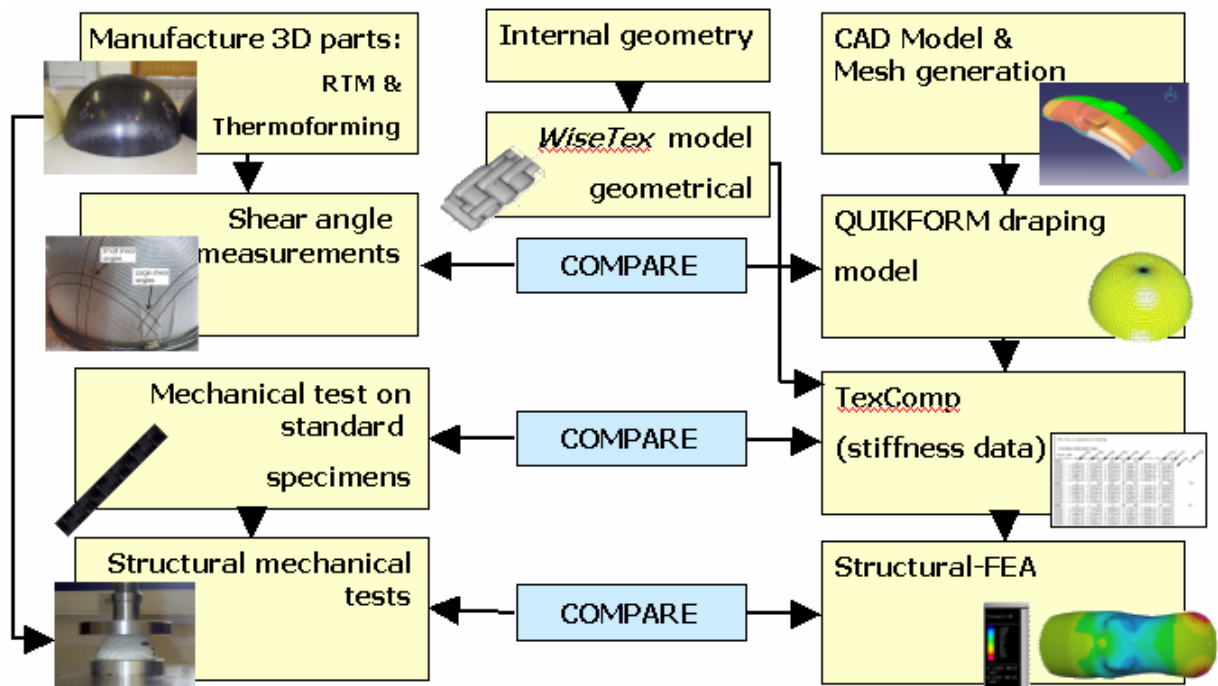


Figure 1. Micro-Macro mechanical modelling approach

The software package *WiseTex* [1] is used to generate a geometrical model for a Representative Volume Element (RVE) of a sheared textile structure, based on results of the draping simulation with a kinematical *QuikForm* software [2]. The geometry of the RVE is then used by micro-mechanical model *TexComp* (method of inclusions [1, 3]) to calculate the local stiffness properties, which are used as input in structural finite element analysis with *SYSPLY* package [2]. The paper describes an application of the whole simulation cycle to four composite parts.

2 PARTS

The different parts (Table 1 and Figure 2) are modelled with commercial CAD software packages providing a geometrical description. The geometrical models are transferred to a FE mesh that is needed for further simulations.



Figure 2 Composite parts

Table 1 Composite parts

Material	Shape	Dimensions
Woven Glass/ PP (Twintex ®), one layer	Hemisphere	D 100 mm
	Freeform (motorbike mudguard)	400x150x100 mm
Woven glass/epoxy (6 layers)	Hemisphere	D 400 mm
NCF carbon/epoxy (6 layers)		

The reinforcement fabrics were characterised using optical microscopy of the cross-sections for the woven fabrics and the results of study of the internal geometry of non-crimp fabric [4]. Results of the characterisation were used as input for *WiseTex* modelling (Table 2, Table 3, Figure 3).

Table 2 Parameters of woven reinforcements

Parameter		Twintex	Woven glass fabric
Weaving pattern		Twill 2/2	Plain
Yarn width, mm	Warp	4,94±0,03	2,54
	Weft	2,99±0,08	2,54
Yarn spacing, mm	Warp	5,42±0,08	2,78(3,597)
	Weft	2,49±0,12	2,94(3,401)
Yarn thickness, mm	Warp	0,81±0,04	0,23
	Weft	0,44±0,03	0,23
Cross-section geometry		Lenticular	Lenticular
Linear density, tex	Warp	2256	600
	Weft	1128	600

Table 3 Parameters of NCF

Parameter		Value
Number of plies		2
Orientation of the plies		± 45
Areal density, g/sq m		309,9
Fabric thickness, mm		1,070
Stitching pattern		Tricot
Stitching spacing, mm	A	4,94
	B	1,71

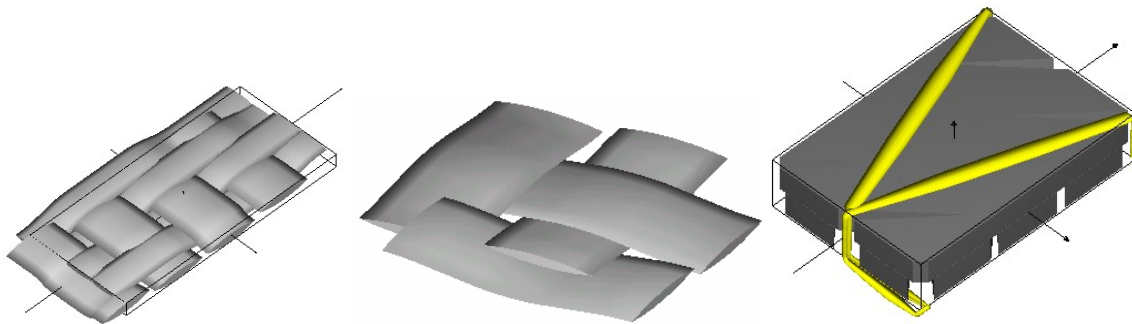


Figure 3 WiseTex models of the reinforcements: Twintex, glass woven fabric, NCF

3 RESULTS

3.1 Draping

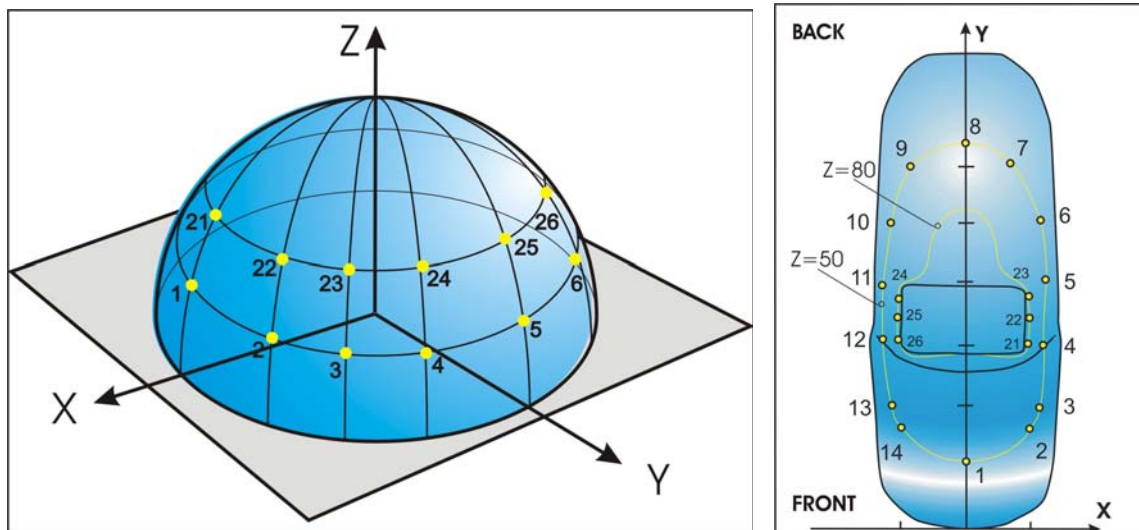


Figure 4 Measurement points on emispherical and mudgard parts

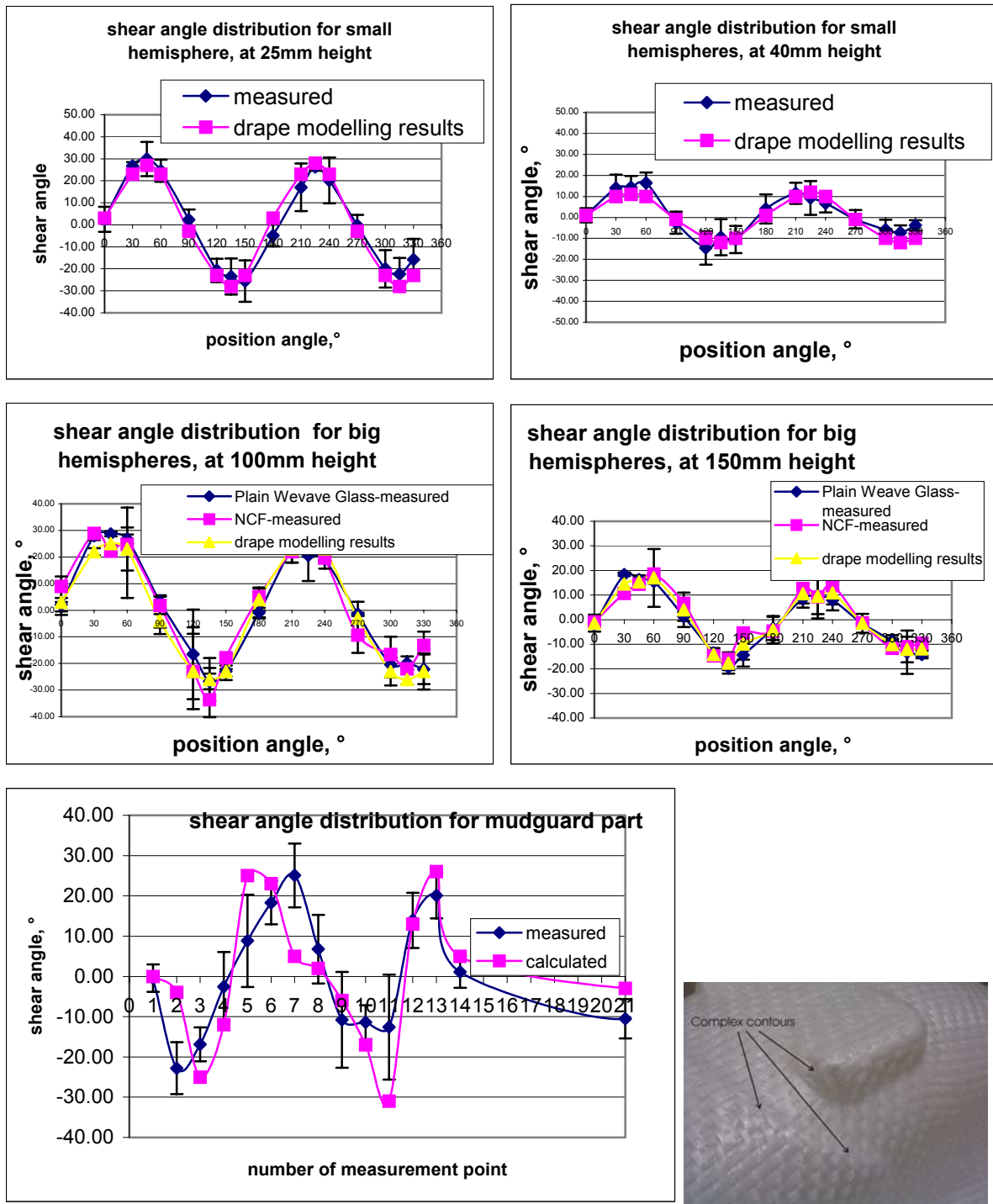


Figure 5 Shear angle of the reinforcement on the parts and locations of highest shear on the mudguard

Local shear angles of the reinforcement on the parts were determined by the direct measurement of the angle between fibres of surface of the parts in points, symmetrically placed on the parts (Figure 4). The errors of this measurement are estimated not to be greater than 2...3°.

Although a kinematical draping algorithm is used and hence the material properties are not taken into account during the simulation, the prediction of the textile deformation is relatively accurate (Figure 5). Deviations occur especially in areas where the curvatures of the part change rapidly (as in the mudguard part), and where the shear angles are highest.

3.2 Local stiffness

The local stiffness of the parts was calculated as follows (Figure 6). *QuikForm* output file contains shear angles of the reinforcement in all the elements of the mesh (the difference between shear of the different layers of the preform was neglected). For each element *WiseTex* calculated the internal geometry of the sheared reinforcement. The result was processed by *TexComp* to produce full stiffness matrix of the impregnated reinforcement in the element in the coordinate system, appropriate for different software tools. This calculation therefore accounts for the differences of the properties in elements of the mesh induced by local shear: (1) fibre volume fraction; (2) in-plane orientations of the yarns and fibres inside them; (3) out-of-plane orientations of the yarns in the sheared woven structure. Note that these factors are predicted by *WiseTex* model with more accuracy than by a simplistic model of change of in-plane fibre directions according to the shear angle.

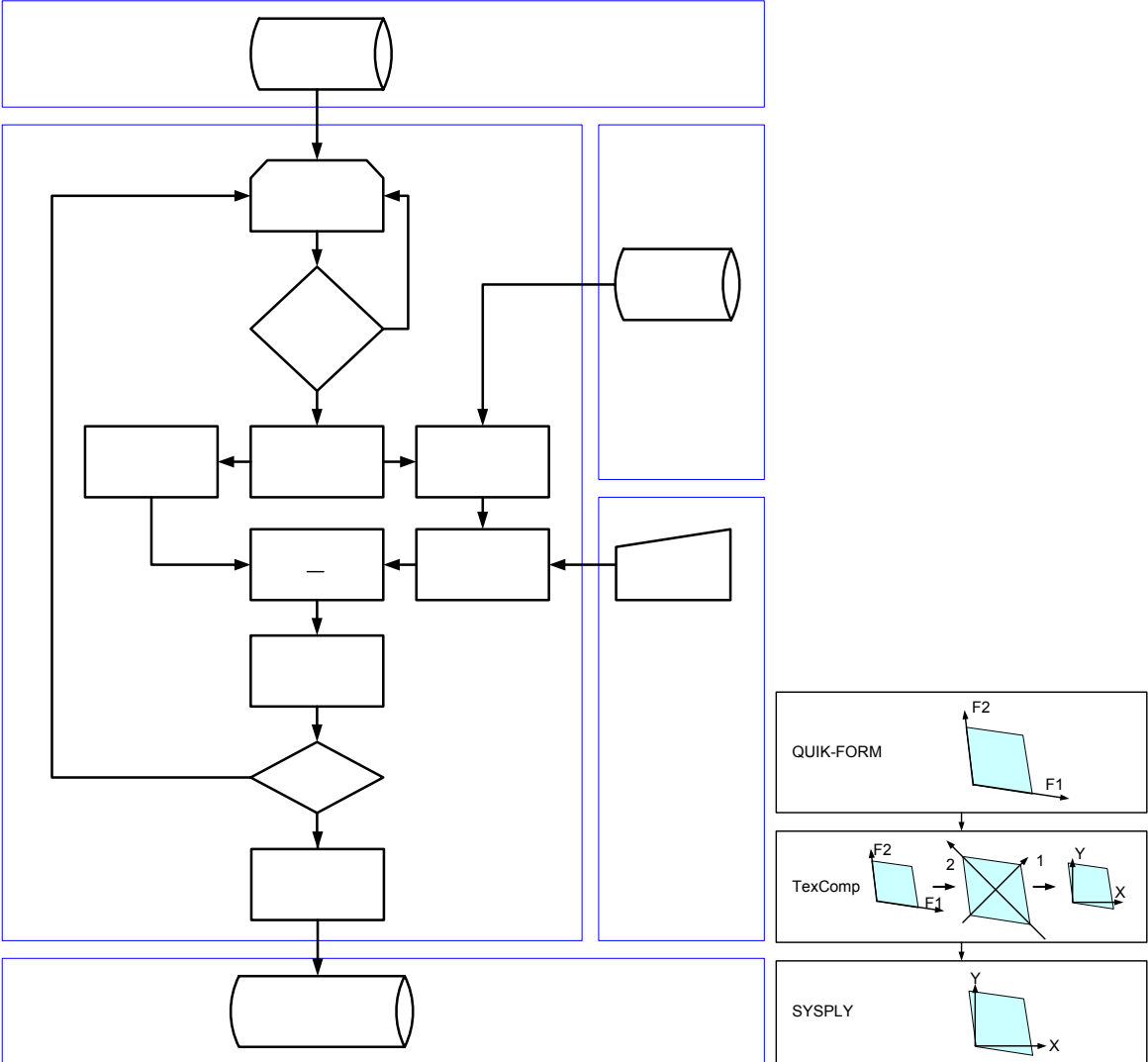


Figure 6 Data flow for calculation of local stiffness of finite elements and coordinate systems in different software tools

3.3 Static part testing

The parts were tested in compression at the constant rate of 1 mm/min. Test set-up has to be chosen carefully to establish the same boundary conditions for tests and simulations. No

translation and no rotation are easy to model in FEA and these boundary conditions will be realised in the test set-up.

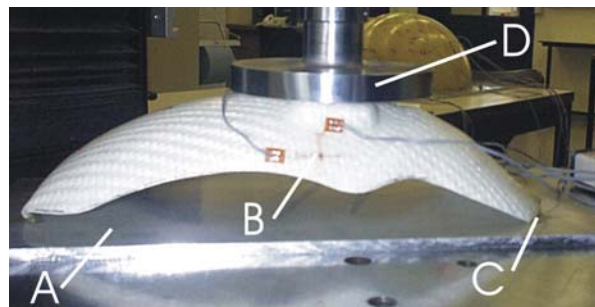
For the small hemispheres it is a straightforward choice to load the parts from the top. To support the part a plate with a groove is made (Figure 7). The small hemispheres are glued in the groove with epoxy so no movement of the part is allowed anymore. It can be assumed the boundary conditions for this part are: no translations and no rotations of the glued-in part (bottom nodes of the virtual model). A hole was drilled into the support plates so entrapped air could escape during the test.

The big hemispheres were also loaded from the top. For the hemispheres in glass fibre and the hemispheres in carbon fibre the same approach was used. The support plate was a simple aluminium plate of 8 mm thickness where the big hemispheres were glued on. No translations and no rotations are allowed anymore on the line where the part is glued to the plate.

Also the mudguard part was loaded from the top. The same technique is applied as with the big hemispheres: the parts are glued onto the aluminium support plates with glue. The part is glued at the front over 13 mm and back tip over 7 mm so these nodes in the virtual model will be locked in translation and rotation. This condition was not exactly followed in the actual testing (Figure 7).



Figure 7 Top left: fracture on a big hemisphere; Top right: A compressed small hemisphere; Bottom right: Load set-up of the mudguard. A: The support plate; B: strain gauge; C: gluing the part on the support plate; D: The load head. Note deformations at the points C



All parts are glued on the support plates with Araldite 2100 glue. Araldite 2100 can be processed a long time so it makes it easy to glue big surfaces. To improve the adhesion on the plates for the big hemispheres and the mudguards their support plates were treated with sandpaper and degreased with acetone afterwards. The glue cured at least for ± 24 hours before tests where started.

Attention has to be paid to choose the length of the strain gauges comparable with the size of a unit cell of the fabric. This has as a result that fluctuations of properties inside a unit cell are averaged. Two kinds of strain gauges are used during the tests¹ – Table 4.

Table 4 Strain gauges used during the tests.

	Type	Gauge length	Gauge resistant	Gauge factor	
	-	mm	Ω	%	%
Biaxial	PC-20-11	20	120 ± 0.3	2.12	2.12
Unidirectional	FLA-10-11	10	120 ± 0.3	2.12	

The centres where the strain gauges have to be positioned are first marked. Afterwards the strain gauges are glued on very carefully with cyanoacrylate glue. The strain gauges are always glued a horizontal or vertical way.

Strain gages were placed as follows (see Figure 4 for definition of the points):

Small hemispheres: at positions 1 (biaxial), 7 and 11 (uniaxial)

Big hemispheres:

- Biaxial strain gauges on points 3, 7, 11 and 15
- Two horizontal placed unidirectional strain gauges on points 1 and 9
- Vertically placed unidirectional strain gauges on points 5 and 13

Mudguard: Two biaxial strain gauges at points 25 and 22

First the parts are loaded from the top with a small displacement of the load head so the deformation goes on in the elastic regime. This is done because only 4 input channels are available on the amplifiers. The big hemispheres have 12 strain gauges glued on so we need at least 3 tests to record all values. A 4th test is done to see if the material does not degrade too much during the tests. Afterwards the parts are unloaded and loaded again with a big displacement up to fracture (Figure 7).

3.4 Structural FEA and comparison with the test results

FEA (SYSPLY) was performed using stiffness of the elements calculated with: (1) *WiseTex/TexComp*; (2) simple model based on Classical Laminate Theory and in-plane changes of the fibre orientations.

Boundary conditions in FE models were set as follows. The bottom nodes of the hemispheres are connected to an imaginary point P so they cannot be moved and rotated relatively to this point (no relative rotations or displacements of the nodes). For the mudguard the nodes in the area where the part touched the support plate are connected to this point P (this is over a length of 13 mm in the front and over a length of 7 mm in the back of the part). At the top, the parts are placed against a load plate that is modelled with infinite stiffness. This load plate is fixed. The imaginary point P, is now moved in Z direction over well defined distances and with it, the connected nodes are moved over the same distance. By doing this, the part is compressed like we did in the tests of the real parts. For each movement the response of the part is calculated in the FE model. The response of the FE model includes calculation of properties of elements and properties of nodes. Results of the simulations are stored in a binary file (*.DSY) which can be processed by PAM-VIEW (Figure 8).

¹ All strain gauges used are made by Tokyo Sokki Kenkyujo Co., Ltd.

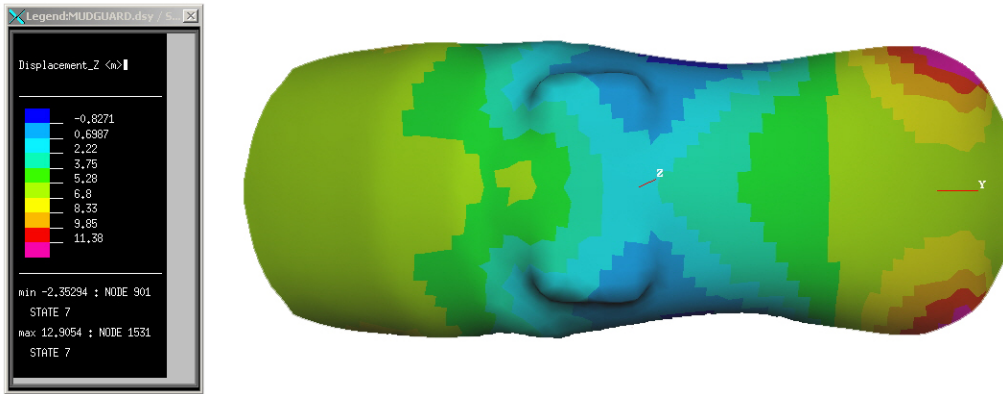


Figure 8 Z-displacements of the mudguard part. Head displacement 6 mm.

From PAM-VIEW the reaction forces at the boundary nodes of the part are extracted. If these values are summed up, the global load on the part for a given displacement is found. The elements where the strain gauges are located are traced and the coordinates of its four nodes, for every state, are extracted from PAM-VIEW. These coordinates are used to calculate the strains of the elements in the same directions as the strain gauges glued on the real parts.

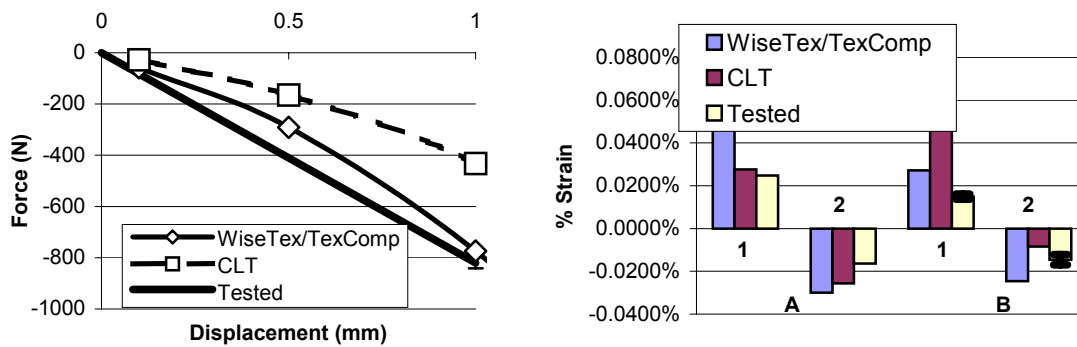


Figure 9 Experimental and calculated load-deflection curves (left) and local strains (right, 1 mm displacement of the compression head). Twintex small hemisphere, 1: strain in horizontal direction, 2: strain in vertical direction. A: low shear positions, B: high shear positions

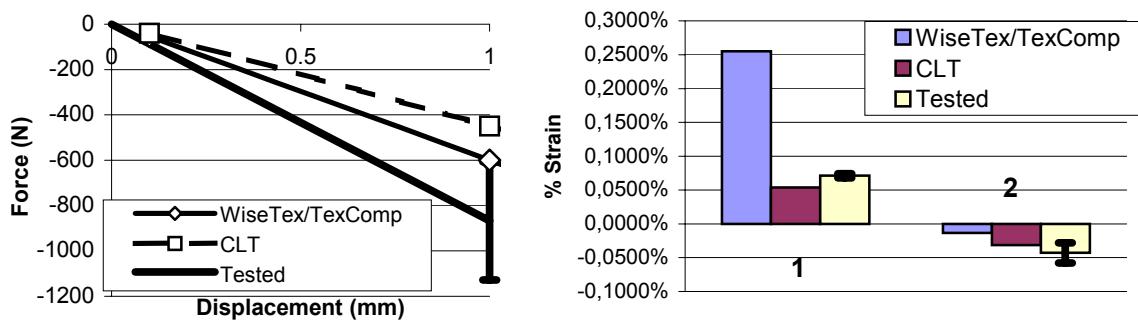


Figure 10 Experimental and calculated load-deflection curves (left) and local strains (right, 1 mm displacement of the compression head). Twintex mudguard, strain in horizontal (1) and vertical (2) directions at a point in the middle of a side of the part.

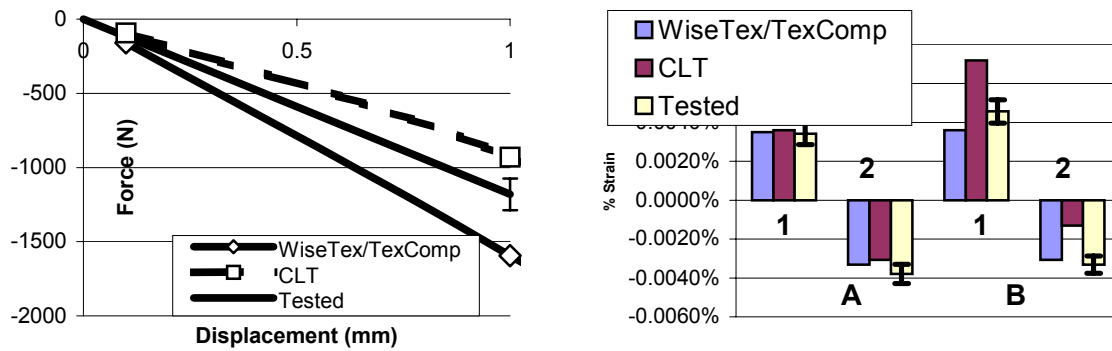


Figure 11 Experimental and calculated load-deflection curves (left) and local strains (right, 1 mm displacement of the compression head). Glass/epoxy large hemisphere, 1: strain in horizontal direction; 2: strain in vertical direction. A: low shear positions, B: high shear positions

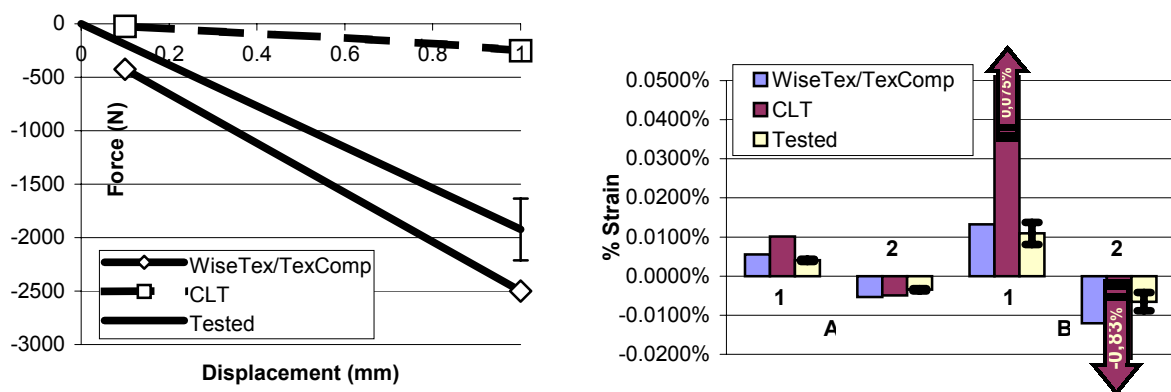


Figure 12 Experimental and calculated load-deflection curves (left) and local strains (right, 1 mm displacement of the compression head). Carbon/epoxy large hemisphere, 1: strain in horizontal direction; 2: strain in vertical direction. A: low shear positions, B: high shear positions

Figure 9 – Figure 12 illustrate the comparison between the experimental and the calculated results for the elastic region of deformation of the parts.

Comparison between the global part behaviour (force-displacement for the whole part) during loading and the FE simulation shows a good prediction of the part stiffness in elastic region. For the local part behaviour (strains on specific points on a part): tension and compression are predicted reasonably close to the measured values, except for the mudguard shaped part. Possible cause of differences lies in a certain difference in the simulated and the actual boundary conditions, as discussed above.

Results also show that the ‘micro-macro modelling’ technique based on the *WiseTex* models approaches the tested values better than the simplified models. This is true for global as well as for local results. The most notable improvement is in areas where textile structures are highly deformed during production (large shearing angle of the fabric), as it could be expected.

4 CONCLUSION

We have demonstrated a good integration in the chain of micro-macro mechanical modelling between the used software tools (*QuikForm* – *WiseTex* – *TexComp* – *SYSPLY*). The integration of micro-macro modelling approach for textile composites has been proven to represent a reality with a reasonable accuracy in the elastic deformation region.

5 ACKNOWLEDGEMENTS

The work reported here has been carried out in the scope of the projects TECABS (funded by EC), "Predictive tools for permeability, mechanical and electro-magnetic properties of fibrous assemblies" (funded by IWT, Flanders), "Concurrent multi-scale design/engineering of textile composites" (funded by Flemish Government via K.U.Leuven). It is largely based on a thesis work of BVDB and FT for a Master degree under EUPOCO program in K.U.Leuven.

6 REFERENCES

1 **S.V.Lomov, G.Huysmans, Y.Luo, R.S. Parnas, A.Prodromou, I.Verpoest, F.R. Phelan**, Textile composites: Modelling strategies, *Composites A*, vol. **32**, N 10, 1379-1394, 2001

2 <http://www.esi-group.com/SimulationSoftware/>

3 **G. Huysmans, I. Verpoest, P. Van Houte**, A poly-inclusion approach for the elastic modelling of knitted fabric composites *Acta Mater*, Vol. 46, No. 9, 1998, pp.3003-3013

4 **S.V.Lomov, E.B.Belov, T.Bischoff, S.B.Ghosh, T.C.Thanh, I.Verpoest**, Carbon composites based on multi-axial multi-ply stitched preforms. Part 1: Geometry of the preform, *Composites A*, vol 33, N9, 2002, 1171-1183